NASA TECHNICAL NOTE

NASA TN D-4934

NASA TN D-4934

C.1

STABILITY ANALYSIS FOR UNLOADED EXTERNALLY PRESSURIZED GAS-LUBRICATED BEARINGS WITH JOURNAL ROTATION

by David P. Fleming, Robert E. Cunningham, and William J. Anderson

Lewis Research Center
Cleveland, Ohio

NATIONAL AERONAUTICS AND SPACE ADMINISTRATION • WASHINGTON, D. C. • DECEMBER 1968

STABILITY ANALYSIS FOR UNLOADED EXTERNALLY PRESSURIZED GAS-LUBRICATED BEARINGS WITH JOURNAL ROTATION

By David P. Fleming, Robert E. Cunningham, and William J. Anderson

Lewis Research Center
Cleveland, Ohio

NATIONAL AERONAUTICS AND SPACE ADMINISTRATION

For sale by the Clearinghouse for Federal Scientific and Technical Information
Springfield, Virginia 22151 – CFSTI price $3.00

ABSTRACT

A small eccentricity analysis was performed for a bearing with two feeding planes, each of which is assumed to be a line source. Numerical results were obtained for a range of bearing number, pressure ratio, feeding parameter, and orifice recess volume. A digital computer program was written to obtain these results and is included. Steady-state load and attitude angle were obtained, as well as stability data. Stability decreased markedly with increasing recess volume; moreover, for large recess volume and low bearing number, an increase in pressure ratio decreased stability. There was no correlation between stability and steady-state attitude angle for any of the cases studied. Fair agreement was obtained with available experimental data.

STABILITY ANALYSIS FOR UNLOADED EXTERNALLY PRESSURIZED GAS-LUBRICATED BEARINGS WITH JOURNAL ROTATION

by David P. Fleming, Robert E. Cunningham, and William J. Anderson

Lewis Research Center

SUMMARY

A small eccentricity analysis was performed to predict the stability of an externally pressurized gas-lubricated journal bearing with two feeding planes, each of which is assumed to be a line source. Numerical results were obtained for a representative range of bearing number, pressure ratio, feeding parameter, and orifice recess volume. These results were obtained by using a digital computer program which is presented in an appendix. Steady-state load and attitude angle were obtained, as well as stability data. Stability decreased markedly with increasing recess volume; moreover, for large recess volume and low bearing number, an increase in pressure ratio decreased stability. There was no correlation between stability and steady-state attitude angle for any of the cases studied. Fair agreement was obtained with available experimental data.

INTRODUCTION

Self-excited instability is one of the severest problems encountered in operating gas-lubricated journal bearings. At high speeds and low loads, the journal may precess about its steady-state position at a frequency which, for a self-acting bearing, is usually about one-half of the frequency of rotation. Hence, this phenomenon has become known as half-frequency whirl. In bearings other than the plain self-acting bearing, particularly in the externally pressurized bearing, the whirl frequency can be considerably different than one-half of the rotational frequency. Therefore, the phenomenon is more properly called fractional frequency whirl. Since fractional frequency whirl is excited by forces generated within the fluid film of the bearing, it is not possible to eliminate it by increasing speed, as is the case with a synchronous resonant condition. Any attempt to increase speed once fractional frequency whirl has begun usually results in rubbing contact between the journal and the bearing.

A major part of the research in gas-lubricated bearings has been directed toward development of bearing configurations that will operate stably when the load is small or zero. Three designs have received primary consideration: herringbone-grooved, tilting-pad, and externally pressurized bearings.

(1) Herringbone-grooved bearing. Shallow helical grooves are cut in either the journal or the bearing to create an inward-pumping viscous pump. This type of bearing shows good promise for operating stably to high speeds (ref. 1), but clearances must be kept very low, approximately 0.5×10^{-3} centimeter per centimeter of shaft radius. These low clearances may cause problems at assembly or when thermal distortion is present, and they require extreme cleanliness of the lubricating gas.

(2) Tilting-pad bearing. This is perhaps the most stable type of gas bearing (ref. 2), but the flexures or pivots required for each of the pads increase the complexity of the system and can lead to fatigue or fretting problems in long-term use.

(3) Externally pressurized bearing. This type of bearing operates well at moderate clearances (10^{-3} cm/cm) and has fairly good stability characteristics. The chief disadvantage is the need for a source of lubricant under pressure. However, sufficient pressure may be generated within the system which uses the gas bearings, so that some of the high-pressure gas may be bled off and used for the bearings without imposing severe penalties on cycle efficiency. This is especially true in large systems. In these systems, externally pressurized bearings may be advantageous and even mandatory, because self-acting bearings large enough to support the required load are impractical. This is so because the load capacity of a self-acting bearing is proportional to the square of its diameter, while the load imposed is a function of the rotating mass, which varies as the cube of the rotor diameter.

Startup problems are common to all of these bearing types. Proper selection of bearing materials will minimize these problems. If the rotor can be "floated" by external pressurization before rotation is attempted, however, the materials problems is reduced considerably. This is easily accomplished in the externally pressurized bearing, and it is common practice, even with tilting-pad bearings to include provision for external pressurization at startup (ref. 3). Obviously, the externally pressurized bearing is simpler than the tilting-pad bearing when the latter must be externally pressurized for startup.

Since externally pressurized bearings may be the best choice for some applications, it is important to know the conditions under which these bearings will operate stably. Because of the large number of parameters that may vary in a physical system, it is slow and expensive to rely solely on experimentation to gain needed information, and it becomes extremely desirable to apply analytical techniques to the stability problem.

A previous analysis (ref. 4) predicts stable regions of operation for externally pressurized gas-lubricated bearings operating at finite (nonzero) eccentricities. Account is taken of orifice recess volume, and an attempt is made to account for having a finite num-

ber of orifices rather than a line source, which is usually assumed. However, the method is quite cumbersome and expensive to apply in terms of computer time. In addition, the analysis requires modification to be applicable to bearings in which the lubricant is introduced at more than one axial location.

A need exists, therefore, for a technique that will provide stability information for an unloaded bearing. Pan (ref. 5) has outlined a general method that is applicable to both loaded and unloaded bearings. For the case of an unloaded bearing, the method is quite simple to apply: the only information needed is steady-state operating data for small amplitude constant whirling. On the other hand, Lund (ref. 6) has derived the expressions for the steady-state load and attitude angle for an externally pressurized bearing operating with a small eccentricity.

The analysis of reference 6 may easily be modified to yield a solution for steady whirling, including the effect of orifice recess volume. When this modified analysis is subjected to the stability criteria of reference 5, the regions of stable operation of an externally pressurized bearing are quite easily determined.

The objectives of this report are to (1) combine the methods of references 4 to 6 to obtain a stability analysis for an externally pressurized gas-lubricated journal bearing operating at zero steady-state eccentricity, (2) develop and present a computer program to carry out the analysis, (3) present representative results of the analysis, and (4) compare the analytical results with experimental data.

ANALYSIS

The analysis is accomplished by applying the expressions from reference 4 concerning orifice recess volume to the analysis of reference 6 to obtain solutions for steady circular whirling as in reference 7. These solutions are then subjected to the stability criteria of reference 5. The analysis is presented in its entirety for better unification of the various constituents.

The configuration to be analyzed is that of an externally pressurized gas-lubricated journal bearing that has two circumferential rows of orifices (fig. 1). Although, in practice, there are a finite number of orifices in each of the two rows, in order to make the problem tractable it is assumed that each row can be represented by a line source. The starting point in the analysis is the time-dependent, compressible, isothermal Reynolds equation (ref. 8):

$$\frac{\partial}{\partial x}\left(ph^3 \frac{\partial p}{\partial x}\right) + \frac{\partial}{\partial z}\left(ph^3 \frac{\partial p}{\partial z}\right) = 6\mu\omega R \frac{\partial}{\partial x}(ph) + 12\mu \frac{\partial}{\partial t}(ph) \tag{1}$$

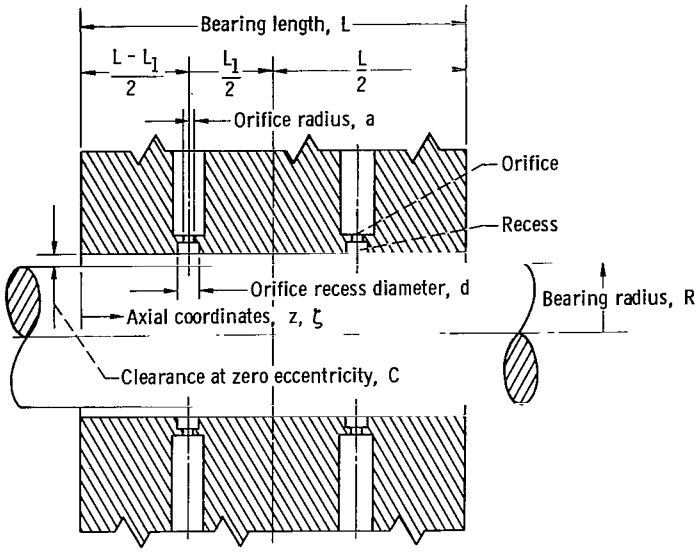

Figure 1. - Geometry of externally pressurized journal bearing.

All symbols are defined in appendix A. This equation may be made dimensionless by using the variables

$$\theta = \frac{x}{R}, \quad \zeta = \frac{z}{R}, \quad P = \frac{p}{p_a}, \quad H = \frac{h}{C}, \quad \tau = \omega_p t \tag{2}$$

Noting that $P(\partial P/\partial x) = (1/2)(\partial P^2/\partial x)$, etc., the dimensionless form of equation (1) is

$$\frac{\partial}{\partial \theta}\left(H^3 \frac{\partial P^2}{\partial \theta}\right) + \frac{\partial}{\partial \zeta}\left(H^3 \frac{\partial P^2}{\partial \zeta}\right) = 2\Lambda \frac{\partial}{\partial \theta}(PH) + 2\sigma \frac{\partial}{\partial \tau}(PH) \tag{3}$$

in which the bearing number Λ is defined by

$$\Lambda = \frac{6\mu\omega}{p_a}\left(\frac{R}{C}\right)^2 \tag{4}$$

and the frequency number σ by

$$\sigma = \frac{12\mu\omega_p}{p_a}\left(\frac{R}{C}\right)^2 = 2\frac{\omega_p}{\omega}\Lambda \tag{5}$$

The following two cases will be considered:

(1) There is no whirling ($\omega_p = \sigma = 0$), but an externally applied load causes the bearing to operate with a small eccentricity ratio ϵ.

(2) There is no external load, but the journal is whirling in a small circular orbit about the bearing center with frequency ω_p.

For both cases there will be a force generated in the fluid film which will tend to move the journal center toward the bearing center.

If the journal and bearing axes are assumed to be always parallel, the dimensionless film thickness H for case 1 is given by

$$H(\theta) = 1 + \epsilon \cos \theta \tag{6}$$

and for case 2 by

$$H(\theta, \tau) = 1 + \epsilon \cos(\theta - \tau) \equiv 1 + \epsilon \cos \theta^* \tag{7}$$

As in reference 7, a rotating coordinate system is introduced by

$$\theta^* \equiv \theta - \tau \tag{8}$$

Then

$$\frac{\partial}{\partial \theta} = \frac{\partial}{\partial \theta^*} \tag{9a}$$

and

$$\frac{\partial}{\partial \tau} = - \frac{\partial}{\partial \theta^*} \tag{9b}$$

For both cases 1 and 2, the Reynolds equation becomes

$$\frac{\partial}{\partial \theta}\left(H^3 \frac{\partial P^2}{\partial \theta^*}\right) + H^3 \frac{\partial^2 P^2}{\partial \zeta^2} = 2(\Lambda - \sigma)\left(H \frac{\partial P}{\partial \theta^*} - P\epsilon \sin \theta^*\right) \tag{10}$$

where, in the last term, $1 + \epsilon \cos \theta^*$ has been substituted for H.

The pressure P may now be represented as a power series in the eccentricity ratio ϵ. For small values of ϵ, it will be sufficient to consider only the first two terms of the series:

$$P(\theta^*, \zeta) \cong P_0(\zeta) + \epsilon P_1(\theta^*, \zeta) \tag{11}$$

If equations (11) and (7) are substituted into equation (10) and the resulting expression is considered an identity in ϵ, a separate equation may be written for each power of ϵ which appears. If powers of ϵ higher than 1 are neglected, two equations result:

$$\frac{\partial^2 P_0^2}{\partial \zeta^2} = 0 \tag{12}$$

$$\frac{\partial^2 (P_0 P_1)}{\partial \theta^{*2}} + \frac{\partial^2 (P_0 P_1)}{\partial \zeta^2} - (\Lambda - \sigma)\left[\frac{1}{P_0}\frac{\partial (P_0 P_1)}{\partial \theta^*} - P_0 \sin \theta^*\right] = 0 \tag{13}$$

Before complete solutions of these equations can be obtained, boundary conditions for P_0 and P_1 must be found.

At the end of the bearing, the film pressure p equals the atmospheric pressure p_a. The conditions on P_0 and P_1 are then

$$P_0 = 1 \quad \text{and} \quad P_1 = 0 \quad \text{at} \quad \zeta = 0 \tag{14}$$

The pressure is symmetric about the bearing midplane; thus,

$$\frac{\partial P_0}{\partial \zeta} = \frac{\partial P_1}{\partial \zeta} = 0 \quad \text{at} \quad \zeta = \xi + \xi_1 \tag{15}$$

where

$$\xi = \frac{L - L_1}{D} \tag{16a}$$

and

$$\xi_1 = \frac{L_1}{D} \tag{16b}$$

With this condition, it is necessary to obtain a solution in only one-half of the bearing. At the feeding planes, the gas flow through the orifice restrictors equals the flow out through

the bearing. The dimensionless mass flow through a single orifice is given by

$$\left.\begin{aligned} \frac{\dot{M}(\mathscr{R}T)^{1/2}}{\pi a^2 P_s p_a} = m = \alpha \left(\frac{2k}{k+1}\right)^{1/2} \left(\frac{2}{k+1}\right)^{1/(k-1)} \qquad & \frac{P_c}{P_s} \leq \left(\frac{2}{k+1}\right)^{k/(k-1)} \\ \frac{\dot{M}(\mathscr{R}T)^{1/2}}{\pi a^2 P_s p_a} = m = \alpha \left(\frac{2k}{k-1}\right)^{1/2} \left(\frac{P_c}{P_s}\right)^{1/k} \left[1 - \left(\frac{P_c}{P_s}\right)^{(k-1)/k}\right]^{1/2} \qquad & \frac{P_c}{P_s} > \left(\frac{2}{k+1}\right)^{k/(k-1)} \end{aligned}\right\} \quad (17)$$

To approximately account for the effect of inherent compensation, Lund (ref. 4) proposed to modify the mass flow in equation (17) by dividing by the factor $\left[1 + (\delta/H)^2\right]^{1/2}$, where $\delta = a^2/dC$ is the "inherent compensation factor."

The orifice recess (fig. 1), which has a volume V_c, can act as a reservoir for the supply gas. The actual mass flow into the bearing from one orifice recess is

$$\dot{M}_b = \dot{M}_c - \frac{p_a V_c \omega_p}{\mathscr{R}T} \frac{\partial P_c}{\partial \tau} \quad (18)$$

in which P_c is the dimensionless pressure in the recess. Since the inherent compensation factor is assumed to be small, the pressure in the bearing adjacent to the orifice recess will be infinitesimally different from the pressure in the recess, and is also denoted by P_c. The dimensional orifice mass flow modified for inherent compensation is denoted by $\dot{M}_c$ and is given by

$$\dot{M}_c = \frac{\pi a^2 P_s p_a}{(\mathscr{R}T)^{1/2}} \frac{m}{\left[1 + \left(\frac{\delta}{H}\right)^2\right]^{1/2}} \quad (19)$$

The Hagen-Poiseulle law gives the flow in the bearing away from the feeding plane. This must equal the flow out of the orifice recesses. Since there are N/2 orifices in each row, equations of mass flow into and out of the bearing yield, per unit of circumference,

$$\frac{N}{4\pi R}\left(\dot{M}_c - \frac{p_a V_c \omega_p}{\mathscr{R}T} \frac{\partial P_c}{\partial \tau}\right) = \frac{P_c H^3 C^3 p_a^2}{12 \mu R \mathscr{R}T}\left(\left.\frac{\partial P}{\partial \zeta}\right|_{\zeta=\xi^-} - \left.\frac{\partial P}{\partial \zeta}\right|_{\zeta=\xi^+}\right) \quad (20)$$

The right side of this expression denotes a discontinuity in the axial derivative of the pressure at $\zeta = \xi$ due to the gas entering the bearing at this point. The mass flow may be expressed in a power series in ϵ in the same way as the pressure. If, again, only powers of ϵ through 1 are retained,

$$\dot{M}_c = \dot{M}_{c0} + \epsilon \left.\frac{\partial \dot{M}_c}{\partial \epsilon}\right|_{\epsilon=0} \tag{21}$$

If one now substitutes the expression found by differentiating equation (19) for $\partial \dot{M}_c/\partial \epsilon$ in equation (21) and then combines equations (7), (11), and (21) with equation (20), an expression results which, again, may be considered an identity in ϵ. If powers of ϵ only through 1 are retained, two equations result

$$q = \left.\frac{\partial P_0^2}{\partial \zeta}\right|_{\zeta=\xi^-} - \left.\frac{\partial P_0^2}{\partial \zeta}\right|_{\zeta=\xi^+} \tag{22}$$

$$\left.\frac{\partial (P_0 P_1)}{\partial \zeta}\right|_{\zeta=\xi^-} - \left.\frac{\partial (P_0 P_1)}{\partial \zeta}\right|_{\zeta=\xi^+} = \frac{q}{2}\left(\frac{1}{m_0}\left.\frac{\partial m}{\partial \epsilon}\right|_{\epsilon=0} - \frac{3 + 2\delta^2}{1 + \delta^2}\cos\theta^*\right) + \sigma\psi_1 \left.\frac{\partial (P_0 P_1)}{\partial \theta^*}\right|_{\zeta=\xi} \tag{23}$$

in which the following definitions are used:

$$q = \Lambda_t m_0 P_s \tag{24}$$

$$\Lambda_t = \frac{6\mu N a^2 (\mathscr{R} T)^{1/2}}{p_a C^3 \left(1 + \delta^2\right)^{1/2}} \tag{25}$$

$$\psi_1 = \frac{N V_c}{\pi D^2 C P_{0c}} \equiv \frac{v}{P_{0c}} \frac{L}{D} \tag{26}$$

To evaluate $\partial m/\partial \epsilon$, one writes

$$\frac{\partial m}{\partial \epsilon} = \frac{\partial m}{\partial\left(\frac{P_c}{P_s}\right)} \frac{\partial\left(\frac{P_c}{P_s}\right)}{\partial \epsilon} = \frac{P_{1c}}{P_s} \frac{\partial m}{\partial\left(\frac{P_c}{P_s}\right)} \tag{27}$$

From equation (17),

$$\left.\begin{aligned} &\frac{\partial m}{\partial\left(\frac{P_c}{P_s}\right)} = 0 \qquad \frac{P_c}{P_s} \le \left(\frac{2}{k+1}\right)^{k/(k-1)} \\ &\frac{\partial m}{\partial\left(\frac{P_c}{P_s}\right)} = \alpha \left[\frac{2}{k(k-1)}\right]^{1/2} \frac{\left(\frac{P_c}{P_s}\right)^{(1-k)/k} - \frac{k+1}{2}}{\left[1 - \left(\frac{P_c}{P_s}\right)^{(k-1)/k}\right]^{1/2}} \qquad \frac{P_c}{P_s} > \left(\frac{2}{k+1}\right)^{k/(k-1)} \end{aligned}\right\} \tag{28}$$

If ψ_0 is defined by

$$\psi_0 = -\frac{\Lambda_t}{2P_{0c}} \left.\frac{\partial m}{\partial\left(\frac{P_c}{P_s}\right)}\right|_{\epsilon=0} \tag{29}$$

boundary condition (23) becomes

$$\left.\frac{\partial(P_0P_1)}{\partial \zeta}\right|_{\zeta=\xi^-} - \left.\frac{\partial(P_0P_1)}{\partial \zeta}\right|_{\zeta=\xi^+} - \sigma\psi_1 \frac{\partial(P_0P_1)}{\partial \theta^*} + \psi_0 P_0 P_1 = -q \frac{\delta^2 + 1.5}{\delta^2 + 1} \cos\theta^* \tag{30}$$

Now that the boundary conditions have been established, the differential equations

can be solved. The solution of equation (12) for P_0 (the concentric solution) is easily obtained as

$$\left.\begin{aligned} P_0^2 &= 1 + q\zeta \qquad \zeta < \xi \\ P_0^2 &= 1 + q\xi \qquad \xi < \zeta < \xi + \xi_1 \end{aligned}\right\} \tag{31}$$

A solution of equation (13) may be obtained by assuming that

$$P_0 P_1 = \mathcal{R}e\left[G(\zeta)e^{-i\theta^*}\right] \tag{32}$$

in which G is a complex function of ζ. If this expression is inserted into equation (13) and it is noted that $\sin\theta^* = \mathcal{R}e\left(ie^{-i\theta^*}\right)$, one obtains, after dividing through by $e^{-i\theta^*}$,

$$G'' - G + i(\Lambda - \sigma)\left(\frac{G}{P_0} + P_0\right) = 0 \tag{33}$$

The primes denote differentiation with respect to the argument ζ. The boundary conditions on P_1 from equations (14), (15), and (30) become, respectively,

$$G = 0 \text{ at } \zeta = 0 \tag{34}$$

$$G' = 0 \text{ at } \zeta = \xi + \xi_1 \tag{35}$$

and

$$G'\Big|_{\xi^-} - G'\Big|_{\xi^+} + (\psi_0 + i\sigma\psi_1)G\Big|_{\xi} = q\,\frac{\delta^2 + 1.5}{1 + \delta^2} \tag{36}$$

The ordinary differential equation (eq. (33)) may now be solved numerically by using a forward integration technique such as Runge-Kutta. The procedure is: Assume a function G_β which satisfies all the conditions for G except that $G'_\beta(0) = \beta$, an arbitrary complex number. Integrate the differential equation (eq. 33)) for G_β from $\zeta = 0$ to $\zeta = \xi$ and apply equation (36). Continue the integration to $\zeta = \xi + \xi_1$ and store the value of $G'_\beta(\xi + \xi_1) = B$. Now assume another function G_γ for which $G'_\gamma(0) = \gamma$ and repeat the above procedure to obtain $G'_\gamma(\xi + \xi_1) = \Gamma$. The linearity of the differential equation

(eq. 33)) allows the use of a linear combination of the two solutions just obtained to yield a third solution which satisfies boundary condition (35). Set $G'(0) = (\beta\Gamma - \gamma B)/(\Gamma - B)$ and a third integration will yield the desired function $G(\zeta)$.

Determination of Load

The radial and tangential forces acting on the bearing may now be determined by integrating the film pressure over the bearing area:

$$\begin{Bmatrix} F_r \\ F_t \end{Bmatrix} = 2\int_0^{L/2}\int_0^{2\pi} p_a P \begin{Bmatrix} -\cos\theta^* \\ \sin\theta^* \end{Bmatrix} R\, d\theta^*\, dz$$

$$= 2R^2 p_a \int_0^{\xi+\xi_1}\int_0^{2\pi} \left[P_0 + \frac{\epsilon}{P_0} Re\left(G\, e^{-i\theta^*}\right)\right] \begin{Bmatrix} -\cos\theta^* \\ \sin\theta^* \end{Bmatrix} d\theta^*\, d\zeta$$

Since P_0 is independent of θ^*, its contribution to the bearing forces will be zero. Performing the rest of the θ^* integration, noting that

$$Re\left(G\, e^{-i\theta^*}\right) = G_{Re} \cos\theta^* + G_{Im} \sin\theta^*$$

(where G_{Re} and G_{Im} are the real and imaginary parts of G, respectively), one has (in dimensionless variables):

$$\begin{Bmatrix} f_r \\ f_t \end{Bmatrix} = \frac{\pi}{2(\xi + \xi_1)} \int_0^{\xi+\xi_1} \begin{Bmatrix} -G_{Re} \\ G_{Im} \end{Bmatrix} \frac{d\zeta}{P_0} = \frac{\pi}{2(\xi + \xi_1)} \begin{Bmatrix} -Re \\ Im \end{Bmatrix} \int_0^{\xi+\xi_1} \frac{G}{P_0}\, d\zeta \qquad (37)$$

The dimensionless forces in equation (37) are defined by

$$\left.\begin{aligned} f_r &= \frac{F_r}{\epsilon p_a LD} \\ f_t &= \frac{F_t}{\epsilon p_a LD} \end{aligned}\right\} \tag{38}$$

Thus, the bearing load components are determined simply as the integral of G/P_0. This integration is conveniently carried out at the same time the differential equation (eq. (33)) is solved. In fact, $\int(G/P_0)\partial\zeta$ may be expressed as a linear combination of $\int(G_\beta/P_0)\partial\zeta$ and $\int(G_\gamma/P_0)\partial\zeta$ and only two integrations of differential equation (33) are necessary. In terms of G_β and G_γ,

$$\begin{Bmatrix} f_r \\ f_t \end{Bmatrix} = \frac{\pi}{2(\xi + \xi_1)(\Gamma - B)} \begin{Bmatrix} -Re \\ Im \end{Bmatrix} \left(\Gamma \int_0^{\xi+\xi_1} \frac{G_\beta}{P_0} d\zeta - B \int_0^{\xi+\xi_1} \frac{G_\gamma}{P_0} d\zeta \right) \tag{39}$$

The bearing radial and tangential load components, which are illustrated in figure 2, are

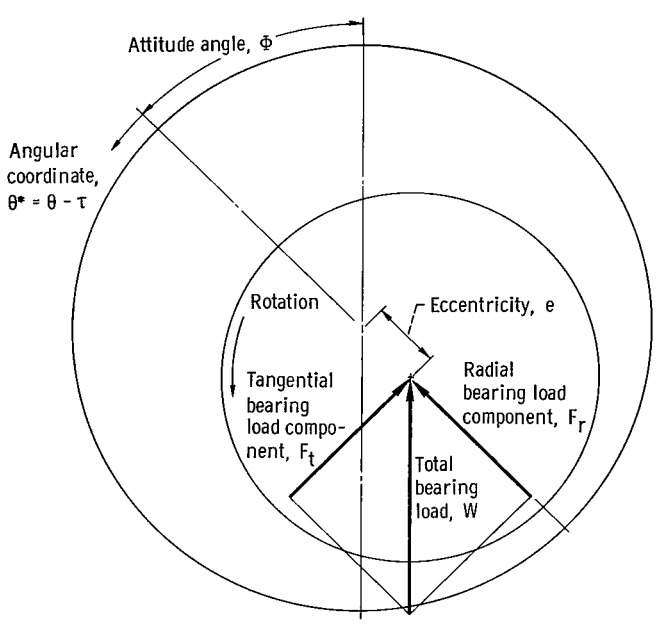

Figure 2. - Notation for eccentric bearing.

now determined as functions of bearing geometry, supply pressure ratio P_s, bearing number Λ, and frequency number σ. The total bearing load

$$W = \left(F_r^2 + F_t^2\right)^{1/2} \tag{40}$$

and attitude angle

$$\varphi = \tan^{-1} \frac{F_t}{F_r} \tag{41}$$

may now be calculated.

Stability Criteria

If the bearing is operating stably, $\sigma = 0$. To determine the threshold of instability, according to the work of Pan (ref. 5), σ is varied until $F_t = 0$. Under this condition, the centrifugal force due to the whirling mass is equated to the radial bearing force to find the neutral stability condition:

$$M\, e\, \omega_{pn}^2 = F_{rn} \tag{42}$$

The subscript n is used to denote the condition where $F_t = 0$. When the bearing is whirling, it is assumed that the flow of gas through the orifice does not vary with time, since the orifices lie behind the recess volume, which acts to dampen flow fluctuations.

A dimensionless mass may be defined by

$$\overline{M}_1 = \frac{Mp_a}{2L\mu^2}\left(\frac{C}{R}\right)^5 \tag{43}$$

In terms of previously calculated quantities, $\overline{M}_1$ for the neutral stability condition is given by

$$\overline{M}_{1n} = \frac{36\, f_{rn}}{\sigma_n^2} \tag{44}$$

It is shown in reference 5 that $\overline{M}_{1n}$ is an upper limit of $\overline{M}_1$ for stability if the quantity $\partial f_t/\partial\sigma$ is negative at $\sigma = \sigma_n$; conversely, $\overline{M}_{1n}$ is a lower limit for stability if $\partial f_t/\partial\sigma$ is positive at $\sigma = \sigma_n$. The definition of $\overline{M}_1$ used herein differs by a factor of 2 from the dimensionless mass used in reference 4; however, it is identical to that used in stability studies of herringbone-grooved gas bearings (refs. 1 and 9).

Another convenient parameter expressing the mass in dimensionless form is

$$\overline{M}_2 = \frac{MC\omega^2}{p_a LD} \tag{45}$$

It is related to $\overline{M}_1$ by

$$\overline{M}_2 = \frac{\Lambda^2}{36}\overline{M}_1 \tag{46}$$

$$\overline{M}_{2n} = f_{rn}\left(\frac{\omega}{\omega_p}\right)^2 \tag{47}$$

Each of these dimensionless masses, $\overline{M}_1$ and $\overline{M}_2$, has its particular advantages. Examination of equation (43) shows that $\overline{M}_1$ depends only on the properties of the bearing and lubricant; it is independent of speed. While $\overline{M}_2$ is a function of speed, it will be seen in the RESULTS AND DISCUSSION section that $\overline{M}_2$ for many bearing configurations is nearly constant for a wide range of Λ.

RESULTS AND DISCUSSION

Numerical results have been obtained for dimensionless load W, attitude angle φ, masses $\overline{M}_{1n}$ and $\overline{M}_{2n}$, and whirl ratio ω_p/ω by using the procedure described in the preceding section. All computations were performed by a high-speed digital computer. The computer program, with sample input and output, is given in appendix B. The bearing configuration chosen has a length-to-diameter ratio L/D of 1.5, with two circumferential feeding planes each located a distance L/4 from the center plane of the bearing; that is, $L_1/D = 0.75$. The inherent compensation factor δ was set at 0.447, which makes $1 + \delta^2 = 1.2$. These values correspond to those of an externally pressurized journal bearing being evaluated experimentally. In reference 10, orifice discharge coefficients are given as a function of the pressure ratio across the orifice and the Reynolds number of the flow. For the conditions encountered in externally pressurized bearings, a reasonable

mean value is 0.7. Accordingly, this value was used in the calculations. Three values of the feeding parameter Λ_t were used: 2, 4, and 10.

Steady-State Results

The steady-state results are identical to those which would be produced by the analysis of reference 6, except for the use of the inherent compensation factor. However, in that reference, no results are given for a bearing with double-plane admission. Inspection of differential equation (33) and boundary conditions (34) to (36) together with the definition of ψ_1 (eq. (26)), shows that the recess volume ratio v enters in only through ψ_1, which appears in equation (36). For steady-state operation, σ, which multiplies ψ_1, is zero, and thus the solution does not depend on v. Accordingly, plots of dimensionless load and attitude angle, in figures 3 and 4, are valid for all values of recess volume ratio.

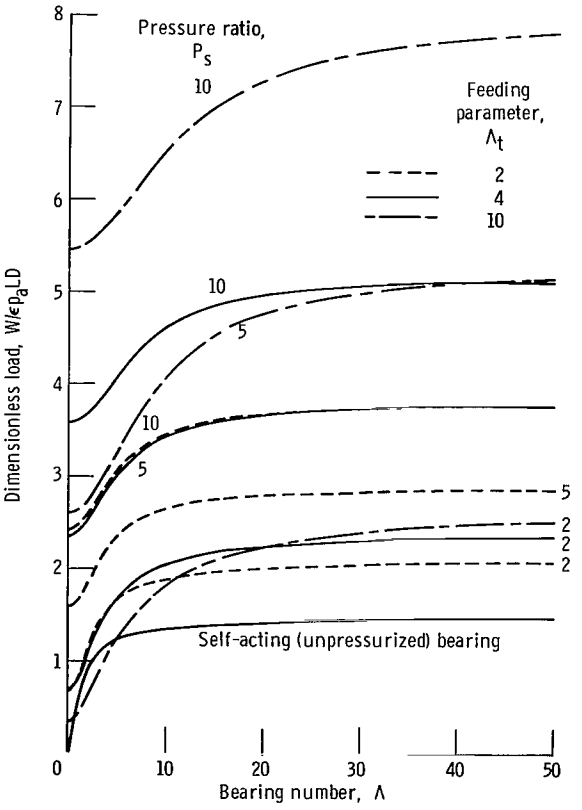

Figure 3. - Steady-state load capacity of externally pressurized bearing. Ratio of bearing length to diameter, 1.5; ratio of distance between feeding planes to bearing diameter, 0.75; orifice discharge coefficient, 0.7; inherent compensation factor, 0.447.

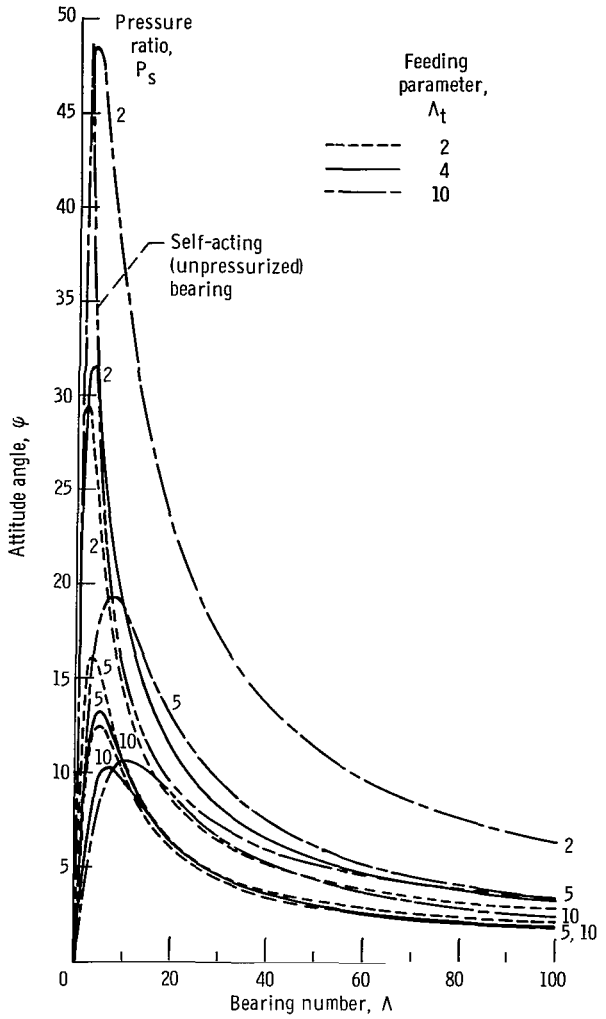

Figure 4. - Steady-state attitude angle for externally pressurized bearing. Ratio of bearing length to diameter, 1.5; ratio of distance between feeding planes to bearing diameter, 0.75; orifice discharge coefficient, 0.7; inherent compensation factor, 0.447.

Figure 3 shows the load capacity increase due to rotational effects. This increase is larger for larger values of the feeding parameter Λ_t, but is relatively insensitive to pressure ratio P_s. For higher values of P_s, however, the zero speed load is higher, so that the total load capacity at all speeds does increase significantly with P_s. For all but the lowest value of P_s, the load capacity of the pressurized bearing exceeds that of the unpressurized, plain bearing. For $\Lambda_t = 10$ and $P_s = 2$, however, the unpressurized bearing carries a higher load than the pressurized bearing for $1/2 < \Lambda < 5$.

Attitude angles are shown in figure 4. The attitude angle φ at zero speed is always zero. Attitude angle increases rapidly with Λ initially, and then falls asymptotically

to zero as $\Lambda \to \infty$. There are three curves in figure 4 which lie partly above that for the plain bearing, indicating that a pressurized bearing does not always have a smaller attitude angle than a self-acting bearing. An increase in pressure ratio always reduces φ, but the behavior with changing Λ_t is not so clearcut. For low pressure ratios and high Λ, φ increases with increasing Λ_t, but the opposite trend appears to occur for low Λ and high P_s.

Stability Results

The dimensionless mass $\overline{M}_{2n}$ is plotted against bearing number Λ in figures 5(a), (b), and (c) for values of Λ_t of 2, 4, and 10, respectively. In each of these figures are curves for P_s of 2, 5, and 10, and recess volume ratios v of 0, 0.2, and 0.4. The curves denote the largest value of $\overline{M}_2$ for which the bearing will be stable.

The most striking feature of the figures is that $\overline{M}_{2n}$ does not vary with Λ when $v = 0$; that is, when there is no orifice recess, the stability as measured by $\overline{M}_{2n}$ is independent of the bearing number. For finite recess volumes, the dependence of $\overline{M}_{2n}$ on Λ becomes stronger as v increases; $\overline{M}_{2n}$ increases with Λ to an intermediate value of Λ, and then decreases. An increase in v always decreases stability.

Another interesting result is that increasing the pressure ratio does not always increase stability, as is commonly assumed. At low values of Λ an increase in pressure ratio may actually decrease stability. This effect is accentuated more and more as the recess volume is increased. The reason is that high pressure ratio and large recess volume are the conditions which promote pneumatic hammer.

A comparison of figures 5(a), (b), and (c) shows that a variation in Λ_t has the same qualitative effect as a variation in P_s; that is, an increase in Λ_t increases stability at low values of v, and decreases stability at high values of v and low Λ.

Some preliminary experimental data from the NASA Lewis externally pressurized test facility are plotted in figure 5(b). The recess volume ratio in the experimental setup was approximately 0.4; other parameters are approximately as shown in figure 5(b). The pressure ratio is indicated next to each plotted point. The experimental points fall approximately where curves would be for $v = 0.1$, except for the point $P_s = 2.2$, which is lower, and, in fact, close to the line $v = 0.4$. Agreement can generally be considered fair. Part of the discrepancy between analysis and experiment could well be due to the number of orifices in the test apparatus. Whereas the analysis assumes a line source, there are, in fact, only six orifices in each row in the experimental setup. This could well reduce the effect of the large recess volume.

The experimental apparatus contains two externally pressurized bearings with a relatively short span. Consequently, when the rotor became unstable, it whirled in a conical

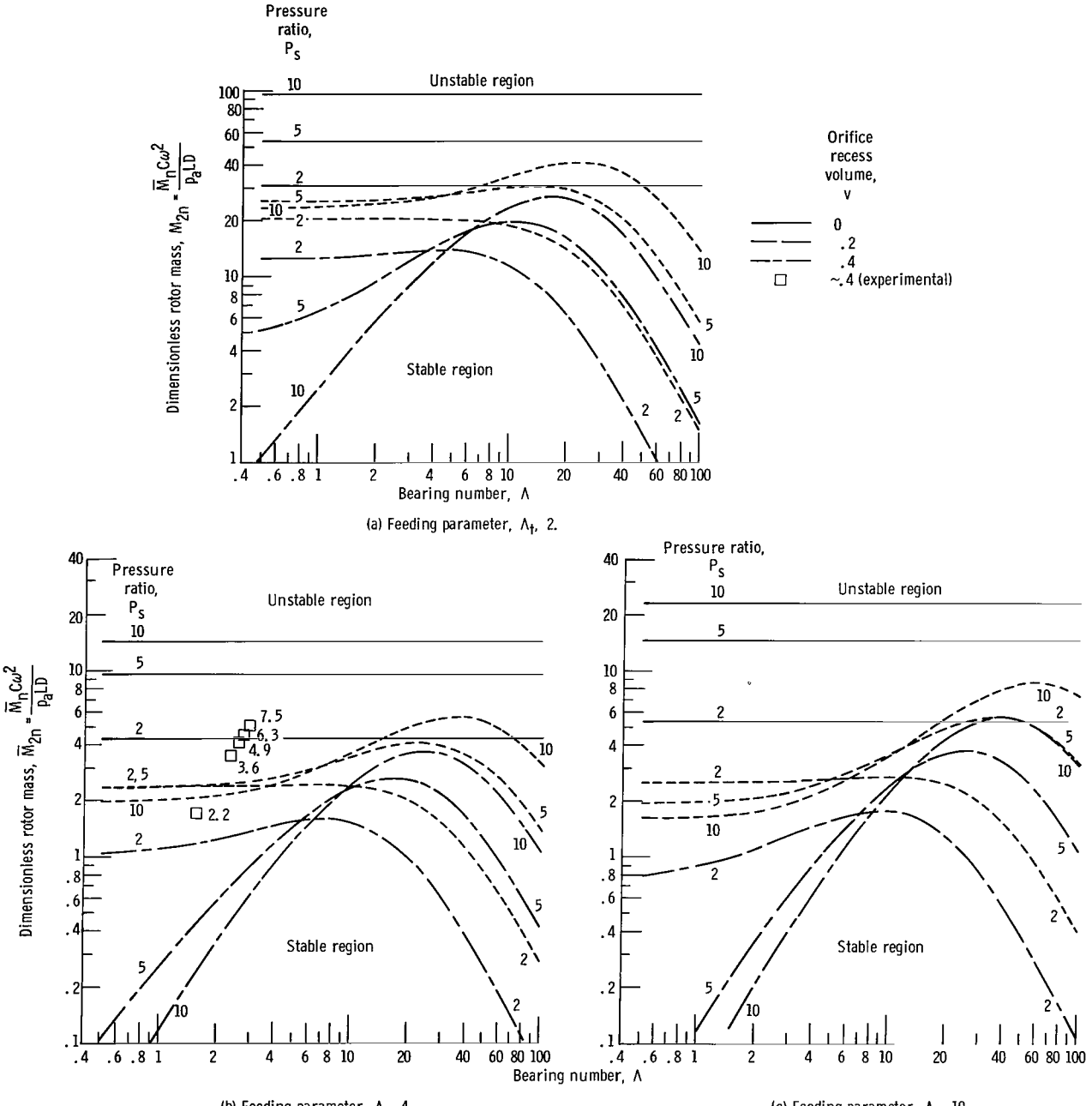

(a) Feeding parameter, Λ_t, 2.

(b) Feeding parameter, Λ_t, 4.

(c) Feeding parameter, Λ_t, 10.

Figure 5. - Stability limits of dimensionless rotor mass $\bar{M}_{2n}$ for externally pressurized bearing. Ratio of bearing length to diameter, 1.5; ratio of distance between feeding planes to bearing diameter, 0.75; orifice discharge coefficient, 0.7; inherent compensation factor, 0.447.

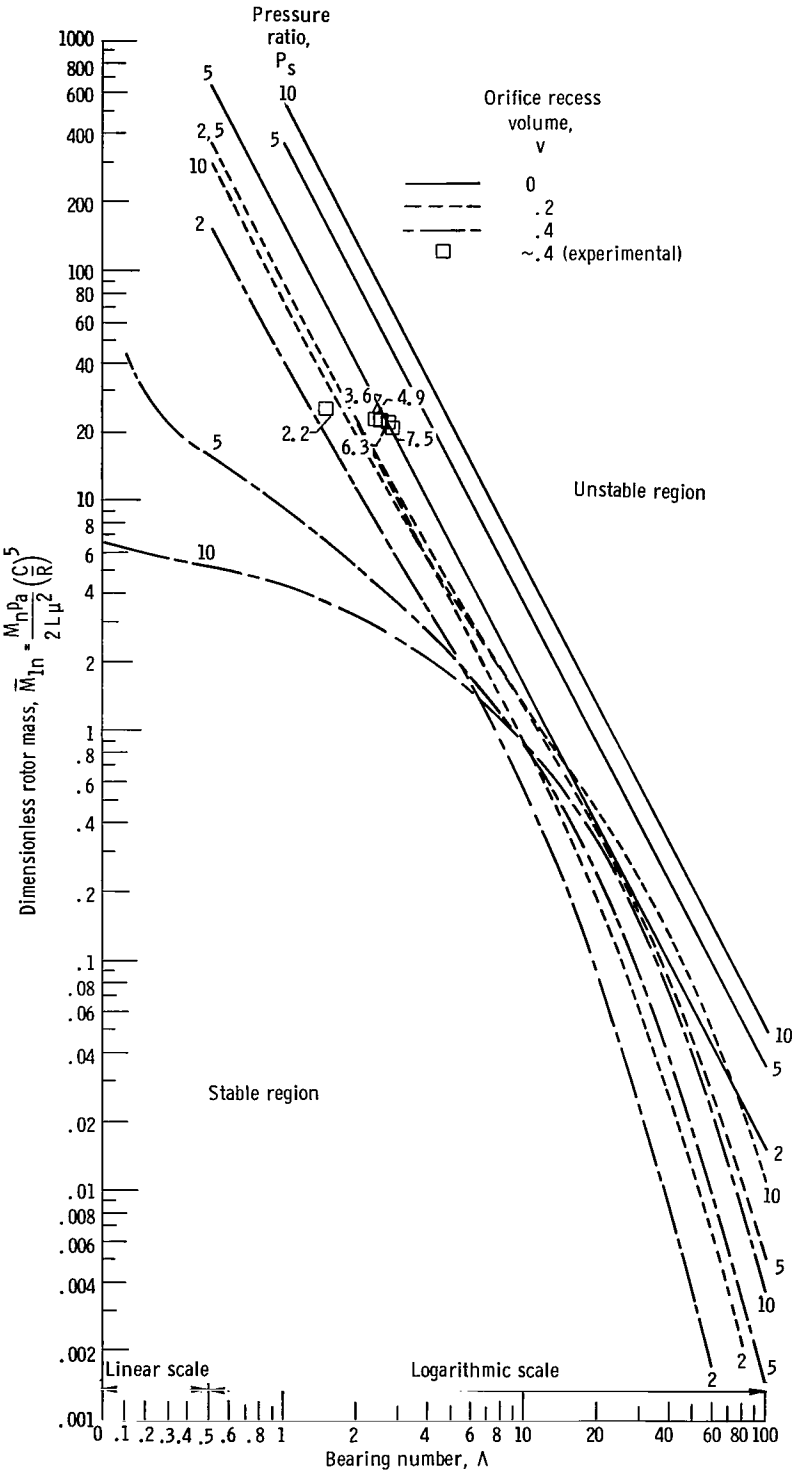

Figure 6. - Stability limits of dimensionless rotor mass $\bar{M}_{1n}$ for externally pressurized bearing. Ratio of bearing length to diameter, 1.5; ratio of distance between feeding planes to bearing diameter, 0.75; orifice discharge coefficient, 0.7; inherent compensation factor, 0.447; feeding parameter, 4.

mode. The mass which was used in the experimental values of $\overline{M}_{2n}$ was an "equivalent mass for conical whirl" defined by

$$M_{eq} = \frac{4(I_{tr} - I_p)}{l^2}$$

wherein I_{tr} and I_p are the transverse and polar mass moments of inertia, respectively, and l is the bearing span. This form is suggested by the solutions to the equations of motion of a rigid rotor presented in reference 11.

The data of figure 5(b) have been replotted in figure 6 with $\overline{M}_{1n}$ as the ordinate instead of $\overline{M}_{2n}$. As already mentioned, $\overline{M}_1$ has the advantage that its definition does not include speed, so that in a given physical setup it remains constant, except for the variation in clearance due to centrifugal force. The experimental points of figure 5(b) are also replotted, and the change in $\overline{M}_1$ due to centrifugal growth of the rotor is evident.

The abscissa has been extended from $\Lambda = 0.5$ to $\Lambda = 0$ on a linear scale. For a pressure ratio of 10 and recess volume ratio of 0.4, $\overline{M}_{1n}$ remains finite for $\Lambda = 0$, indicating a susceptibility to pneumatic hammer. For the lower pressure ratios and recess volume ratios, $\overline{M}_{1n} \to \infty$ as $\Lambda \to 0$, indicating that the bearing is inherently stable when there is no rotation. The tendency toward pneumatic hammer may also be deduced from figure 5. If $\overline{M}_{2n}$ approaches a finite value as $\Lambda \to 0$, there will be no hammer. On the other hand, if $\overline{M}_{2n} \to 0$ as $\Lambda \to 0$, $\overline{M}_{1n}$ remains finite as $\Lambda \to 0$, and pneumatic hammer is possible.

The curves of figures 5 and 6 indicate the heretofore largely unrecognized importance of recess volume in journal bearings. Within the range of variables plotted, changes in v cause larger changes in stability limits than do pressure ratio or feeding parameter. In the design of bearings where instability may be a problem, therefore, it is essential that the recess volume ratio be minimized.

According to the analysis, the instability will occur at some characteristic frequency. For finite Λ, this frequency may be conveniently expressed as a whirl ratio ω_p/ω. Figure 7 illustrates the characteristic whirl ratios corresponding to the stability curves of figures 5(b) and 6. When the recess volume is zero, the whirl ratio is always 0.5, or "half frequency." Whirl ratio ω_p/ω increases with increasing v, and decreases with decreasing Λ, approaching $\omega_p/\omega = 0.5$ as $\Lambda \to \infty$. For the case of pneumatic hammer, $\omega = \Lambda = 0$ and, of course, $\omega_p/\omega = \infty$. Thus, the values for $P_s = 10$ and $v = 0.4$ in figure 7, becoming large for small Λ, indicate again that hammer may be a problem for this configuration.

Experimental values are also plotted in figure 7. Again, the pressure ratio is indicated next to each plotted point. These points bear the same relation to the analytical curves as in figures 5(b) and 6; that is, the experimental points correspond to analytical curves for smaller values of v than were measured.

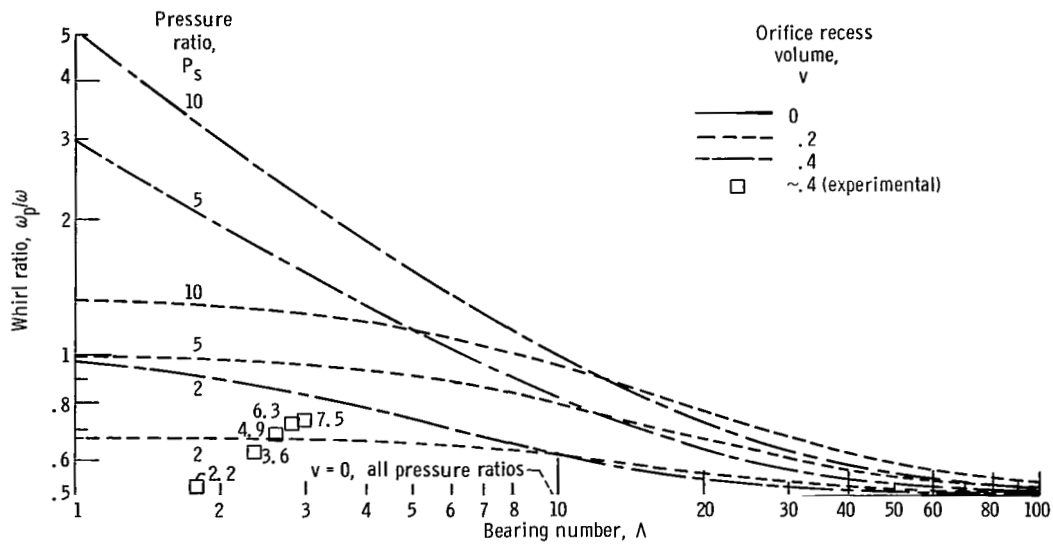

Figure 7. - Frequency of instability. Ratio of bearing length to diameter, 1.5; ratio of distance between feeding planes to bearing diameter, 0.75; orifice discharge coefficient, 0.7; inherent compensation factor, 0.447; feeding parameter, 4.

Relation Between Attitude Angle and Stability

It is popularly assumed that the steady-state attitude angle is a measure of the stability of a fluid-film bearing, a low attitude angle indicating a stable bearing, and a high attitude angle a potentially unstable bearing (ref. 12). This is definitely not the case for the externally pressurized gas-lubricated bearing studied in this report, as an examination of figures 4 to 6 will show.

To eliminate the effect of variable recess volume, at first only the stability curves for $v = 0$ will be considered. Looking at the variation with Λ, one sees that, for all values of pressure ratio and feeding parameter, φ first increases with Λ and then decreases asymptotically to zero, while $\overline{M}_{1n}$ decreases continuously and $\overline{M}_{2n}$ remains constant. Thus, correlation between φ and stability is essentially nonexistent. Now, consider the variation with feeding parameter Λ_t. Stability increases with Λ_t, while at low pressure ratios φ also increases with Λ_t. At higher pressure ratios, the behavior of φ with Λ is anomalous. A plain (unpressurized) bearing, corresponding to $\Lambda_t = 0$, has an attitude angle lower than that for some pressurized bearings, except at very low Λ, and yet the plain bearing is always inherently unstable. When pressure ratio is considered, the attitude angle decreases with increased P_s while stability does increase. However, if now recess volumes other than zero are considered, stability does not always increase with increasing P_s. One concludes that attitude angle is a very unreliable predictor of stability.

SUMMARY OF RESULTS

A small eccentricity stability analysis has been performed for an externally pressurized gas-lubricated bearing that has two feeding planes, each of which is considered to be a line source. A computer program was written to implement the analysis. The following results were obtained for a bearing having a length-to-diameter ratio of 1.5 with two feeding planes located midway between the center and ends of the bearing (quarter plane admission):

1. Stability decreases markedly with increasing recess volume.

2. There is no correlation between stability and steady-state attitude angle.

3. With large recess volumes and low bearing numbers, an increase in pressure ratio may decrease stability. For sufficiently high recess volumes and pressure ratios, pneumatic hammer is possible.

4. The increase in steady-state load capacity due to rotation increases with increasing feeding parameter but is relatively insensitive to pressure ratio; however, total load capacity does increase with increasing pressure ratio.

5. When the orifice recess volume is zero, the dimensionless mass $\overline{M}_{1n}$ does not vary with bearing number Λ.

6. Steady-state attitude angles are sometimes larger than those in plain (unpressurized) bearings.

7. The whirl ratio at the threshold of instability is always 0.5 when the recess volume is zero. Whirl ratio increases with increasing recess volume, but approaches 0.5 asymptotically at large bearing numbers.

8. Preliminary experimental data are in fair agreement with the analytical results.

Lewis Research Center,
National Aeronautics and Space Administration,
Cleveland, Ohio, September 5, 1968,
129-03-13-05-22.

APPENDIX A

SYMBOLS

a	orifice radius
C	clearance at zero eccentricity
D	bearing diameter
d	orifice recess diameter
e	eccentricity
F	bearing load component
f	dimensionless load component, $F/\epsilon p_a LD$
G	dimensionless complex function of ζ
H	dimensionless clearance, h/C
h	local film thickness
I_p, I_{tr}	rotor polar and transverse mass moments of inertia
i	$\sqrt{-1}$
k	specific heat ratio
L	bearing length
L_1	distance between feeding planes
l	bearing span
M	rotor mass per bearing
$\dot{M}$	lubricant flow rate
$\overline{M}_1$	dimensionless rotor mass, $\left(MP_a/2L\mu^2\right)(C/R)^5$
$\overline{M}_2$	dimensionless rotor mass, $MC\omega^2/p_a LD$
m	dimensionless lubricant flow rate, $\dot{M}(\mathscr{R}T)^{1/2}/\pi a^2 P_s p_a$
N	number of orifices per bearing
P	dimensionless pressure, p/p_a
P_1	perturbed pressure
p	pressure
p_a	atmospheric pressure
q	$\Lambda_t m_o P_s$
R	bearing radius
$\mathscr{R}T$	gas constant times absolute temperature
t	time
V_c	orifice recess volume
v	orifice recess volume ratio, $NV_c/\pi DLC$
W	total bearing load
x	coordinate in direction of motion
z	axial coordinate
α	orifice (discharge) coefficient
β, γ	complex values of $G'(0)$
B, Γ	complex values of $G'(\xi + \xi_1)$
δ	inherent compensation factor, a^2/dC
ϵ	eccentricity ratio, e/C
ζ	dimensionless axial coordinate, z/R
θ	angular coordinate
θ^*	angular coordinate, $\theta - \omega_p t$
Λ	bearing number, $6\mu\omega(R/C)^2/p_a$

Λ_t feeding parameter, $\left[6\mu Na^2(\mathscr{R}T)^{1/2}\right] \Big/ p_a C^3\left(1+\delta^2\right)^{1/2}$

μ lubricant dynamic viscosity

ξ $(L - L_1)/D$

ξ_1 L_1/D

σ frequency number, $12\mu\omega_p(R/C)^2/p_a$

τ dimensionless time, $\omega_p t$

φ attitude angle

ψ_0 $-(\Lambda_t/2P_{0c})\left[\partial m/\partial(P_c/P_s)\right]\Big|_{\epsilon=0}$

ψ_1 $NV_c/\pi D^2 C P_{0c}$

ω rotational speed

ω_p frequency of whirling

Subscripts:

b condition immediately downstream of orifice recess

c condition immediately downstream of orifice

n condition at which $F_t = 0$

0 zero eccentricity

r radial

s condition upstream of orifice

t tangential

APPENDIX B

COMPUTER PROGRAM TO DETERMINE STABILITY OF EXTERNALLY PRESSURIZED GAS-LUBRICATED JOURNAL BEARING

The program for determining steady-state and stability characteristics of the externally pressurized bearing is written in FORTRAN IV, version 13, for use on the IBM 7094-II digital computer at Lewis Research Center. Minor modifications may be necessary to allow the program to be used with other computing systems.

Program Input

Two variables are set within the program: k, the specific heat ratio of the lubricant gas, and RKEP, an accuracy parameter. As the program operates, the step size in the Runge-Kutta differential equation solver is successively halved until the magnitude of the bearing load varies by less than RKEP times W.

The remainder of the information needed by the program is read from punched cards. One card contains the array of bearing numbers Λ to be used (up to 19 values). A pair of cards shows each configuration to be analyzed. The first of this pair gives geometric and operating parameters; the second gives initial estimates of the frequency number σ, one for each Λ value. Specific formats follow.

Bearing number array card: Format (I4, 19F4.0)

First four-column field: the number of Λ's in the array, integer format, right adjusted.

Succeeding four-column fields: the values of Λ for which calculations are desired, real format (with decimal point).

Geometric configuration card: Format (10F8.0)

Succeeding eight-column fields contain, in real format (with decimal point): $(L - L_1)/D$, L_1/D, Λ_t, P_s, v, α, and $1 + \delta^2$.

Frequency number estimate card: Format (4X, 19F4.0)

First four-column field is not read. Succeeding four-column fields contain, in real format (with decimal point) the initial estimate of frequency number σ, one value for each Λ.

Any number of pairs of geometric configuration and frequency number estimate cards may be used.

Sample program input follows the program listing included at the end of this appen-

dix. The first card, the Λ array, indicates there are 19 Λ values ranging from 0 to 100. This card is followed by the first geometric configuration card, which indicates that $(L - L_1)/D = 0.75$, $L_1/D = 0.75$, $\Lambda_t = 4$, $P_s = 5$, $v = 0.4$, $\alpha = 0.7$, and $1 + \delta^2 = 1.2$. After this card is the first σ estimate card showing initial estimates of σ, which correspond to the Λ array, of 3 to 100. A second configuration card and σ estimate card conclude the sample input.

Program Output

Output consists of two sheets for each configuration: A "working sheet" and a "calculation summary sheet."

The working sheet shows the geometric and operating parameters, trial values for determination of the pressure downstream of the orifices, final value of orifice downstream pressure, ψ_0, ψ_1, and RKEP. For each Λ in the array, there appear, for each trial value of σ: Λ, f_r, f_t, $W/(\epsilon p_a LD)$, $W/\left[\epsilon(P_s - p_a)LD\right]$, φ, $\overline{M}_2$, final Runge-Kutta step size, $\overline{M}_1$, ω_p/ω, and σ. A sample working sheet appears as figure 8. The data appearing thereon were generated from the values shown in the sample input.

The calculation summary sheet again shows the geometric and operating parameters, and, for each Λ of the Λ array: $W/(\epsilon p_a LD)$, φ, ω_{pn}/ω, σ_n, $\overline{M}_{2n}$, and $\overline{M}_{1n}$. Figure 9 shows an example of a summary sheet. Again, the data correspond to those of the sample input. Program execution time for the sample input was 0.9 minute.

```
$IBFTC LPS
      DIMENSION SLAM(20),SW(20),SPHI(20),SW3(20),SCM(20),SSIG(20)
      DIMENSION ACM(20)
      COMMON XI
      COMMON /CRK/ QD, XI1, CG
      COMMON /CDR/ Q, GD
      COMMON /CFUN/ V, LT, ALFA, PCR, K
      COMMON /CHS/ LAMBDA,PSO,PS1,DX,RDX,CMA,VV,W,PHI,CMC,WR,RKEP
      REAL LAMBDA, LT, K
      COMPLEX DX, GD, CG
      DATA EPS/1.E-5/, EPSW/1.E-3/
      K = 1.4
      RKEP = .005
      READ (5,1) IS, (SLAM(I), I = 1, IS)
1     FORMAT (I4,19F4.0)
3     READ (5,5) XI,XI1,LT,V,VC,ALFA,D1
5     FORMAT (10F8.0)
      READ (5,2) (SSIG(I), I = 1, IS)
2     FORMAT (4X,19F4.0)
      VV = V
      WRITE(6,4)
4     FORMAT (1H1/8X, 67HP-PERTURBATION ANALYSIS FOR HYBRID BEARING IN S
     1TEADY CIRCULAR WHIRL )
C  XI=L(OUTBOARD)/D, XI1=L(INBOARD)/D, LT=LAMBDA(T),ALFA=ORIFICE COEFFICIENT
C  V=PS/PA, VC=FEEDER HOLE VOLUME RATIO, D1=1+DELTA**2
C  XI1=0 DENOTES SINGLE PLANE FEEDING
      WRITE (6,6) XI,XI1,LT,D1,K,ALFA,V,VC
6     FORMAT (6HL  L/D 8X,4HL1/D 7X,8HLAMBDA T 4X,10H1+DELTA**2 3X,
     1 7HK=CP/CV 7X,4HALFA 6X,7HV=PS/PA 7X,2HVC /11G12.3)
      PCR = (2./(K+1.))**(K/(K-1.))
      YA = PCR
      WRITE (6,8)
8     FORMAT (20HLSOLVE FOR YA = PC/V/)
      DO 20 I = 1,10
      CALL FUN(YA,DYA,PSO)
      WRITE(6,10) I, YA, DYA
10    FORMAT (I4,4X,2HYA G14.6,3HDYA G14.6)
      IF(ABS(DYA/YA).LE.EPS) GO TO 25
      YA = YA + DYA
20    YA = AMIN1 (YA, .99)
      GO TO 3
25    Q = ((YA*V)**2 -1.)/XI
      QD = Q*(D1 + .5)/D1
      PSO = PSO/(2.*YA*V)
      PS1 = VC*(XI+XI1)/(YA*V)
      WRITE (6,26) YA,PSO,PS1,RKEP
26    FORMAT (9HK   PC/PS G10.3,5H  PSO G10.3,6H   PS1 G10.3,7H   RKDX
     1 25H REDUCED UNTIL ERROR .LE. G10.3)
      DO 300 I=1,IS
      WRITE (6,140)
140   FORMAT (8HK LAMBDA 4X,8HFR/EPALD 3X,8HFT/EPALD 4X,7HW/EPALD 2X,
     1 12HW/E(PS-PA)LD 4X,3HPHI 4X,9HMCW2/PALD 7X,4HRKDX 5X,
     1 12HMPC5/2LR5MU2 1X, 11HWHIRL RATIO 1X,12HVIB NR SIGMA )
      LAMBDA = SLAM(I)
      SIG1 = SSIG(I)
      DS = 2.
```

```
      IF (LAMBDA.GE.15.) DS=4.
      CALL HYST (0.,GIO)
      IF (LAMBDA.EQ.0.) GIO=.25
      SW(I) = W
      SPHI(I) =PHI
      CALL HYST (SIG1, GI1)
      SIG = SIG1
      IF (ABS(GI1/GIO).LE.EPSW) GO TO 299
      DS1 = SIGN (DS, GI1)
      SIG2 = SIG1
      DO 150 J = 1, 20
      SIG2 = SIG2 + DS1
      CALL HYST (SIG2, GI2)
      SIG = SIG2
      IF (ABS(GI2/GIO).LE.EPSW) GO TO 299
      DS2 = SIGN (DS, GI2)
      IF (DS2 - DS1) 220, 210, 220
210   SIG1 = SIG2
150   GI1 = GI2
      GO TO 299
220   DO 235 J = 1, 10
      SIG = (GI2*SIG1 - GI1*SIG2)/(GI2 - GI1)
      CALL HYST (SIG, GI)
      IF(ABS(GI/GIO).LE.EPSW) GO TO 299
      IF (ABS(GI2).GT.ABS(GI1)) GO TO 230
      GI1 = GI2
      SIG1 = SIG2
230   GI2 = GI
235   SIG2 = SIG
299   SW3(I)=WR
      ACM(I) = CMA
      SCM(I)=CMC
      SSIG(I) = SIG
300   CONTINUE
      WRITE(6,4)
      WRITE (6,600) XI,XI1,LT,   D1,K,ALFA,V,VC,YA,PSO,PS1,RKEP
600   FORMAT(1HL 8X,3HL/D 8X,4HL1/D 6X,8HLAMBDA T 4X,10H1+DELTA**2 3X,
     1  7HK=CP/CV 6X,4HALFA/5X,6G12.3//7X,7HV=PS/PA 2X,
     213HCL.VOL.RAT.VC 3X,5HPC/PS 8X,3HPSO 9X,3HPS1 9X,4HRKEP/5X,6G12.3)
      WRITE (6,325) (SLAM(I),SW(I),SPHI(I),SW3(I),SSIG(I),ACM(I),SCM(I),
     1  I=1,IS)
325   FORMAT (/1HL  7X,6HBRG NR 3X,8HBRG LOAD 2X,22HATT ANGLE  WHIRL RAT
     1IO 2X,6HVIB NR 3X,20HSTABILITY PARAMETERS / 8X,6HLAMBDA 4X,
     2  7HW/EPALD 5X,3HPHI 6X,8HW3/OMEGA 4X,5HSIGMA 4X,9HMCW2/PALD 2X,
     3  12HMPC5/2LR5MU2 / (/7X,2G10.3,G11.3,G12.3,2G10.3,G12.3))
      GO TO 3
      END

$IBFTC FUNF
      SUBROUTINE FUN (Y, DY, PSO)
      COMMON XI
      COMMON /CFUN/ V, LT, ALFA, PCR, K
      REAL LT,M,K
      IF(Y.GT.PCR) GO TO 10
      M = ALFA*SQRT(2.*K/(K+1.))*PCR**(1./K)
      PSO = 0.
      GO TO 15
10    T = SQRT(1.-Y**((K-1.)/K))
      TC = SQRT(2.*K/(K-1.))*ALFA
      M = TC*T*Y**(1./K)
```

```
      PSO = -LT*TC/T*(Y**((1.-K)/K) - (K+1.)/2.)/K
15    T = Y*V*V/XI
      F = LT*V*M - Y*T + 1./XI
      DF = V*PSO + 2.*T
      DY = F/DF
      RETURN
      END

$IBFTC HYDST
      SUBROUTINE HYST (SIGMA, GI)
      COMMON XI
      COMMON /CRK/ QD, XI1, CG
      COMMON /CHS/LAMBDA,PSO,PS1,DX,RDX,CMA,V,W,PHI,CMC,WR,RKEP
      COMMON /CDR/ Q, GD
      REAL LAMBDA
      COMPLEX AA,AB,BA,BB,CA,CB,DX,GD,CG,TDX
      CG = PSO
      IF (SIGMA.NE.0.) CG=SIGMA*PS1*(0.,1.)
C  PSO = 0 WHEN BEARING IS WHIRLING
C  PSO=0 MEANS ORIFICE MASS FLOW DOES NOT VARY WITH THETA
      GD = (0.,1.)*(LAMBDA - SIGMA)
      DX = .5*XI
      TDX = 0.
      DO 110 N = 1, 8
      BA = 0.
      BB = (-1.,-1.)
      CALL RKLP (BA,DX,AA,CA)
      CALL RKLP (BB,DX,AB,CB)
      CA = 1.57079633/(XI+XI1)*(AB*CA - AA*CB)/(AB - AA)
      IF (CABS(TDX/CA-1.) .LE. RKEP) GO TO 120
      DX = .5*DX
110   TDX = CA
120   RDX = REAL(DX)
      GR = -REAL(CA)
      GI = AIMAG(CA)
      W = CABS(CA)
      PHI = ATAN2(GI,GR)*57.2957796
      WV = W/(V-1.)
      WR = 1000.
      CMC = 0.
      IF (SIGMA.NE.0.) CMC = 144.*GR/SIGMA**2
      CMA = CMC*LAMBDA**2/36.
      CMS = CMA/(V-1.)
      IF (LAMBDA.NE.0.) WR = .5*SIGMA/LAMBDA
      WRITE (6,145) LAMBDA,GR,GI,W,WV,PHI,CMA,RDX,CMC,WR,SIGMA
145   FORMAT (3G11.3,2G12.4,G11.3,G12.4,4G13.4)
      RETURN
      END

$IBFTC RKLPS
      SUBROUTINE RKLP (GIN,DX,AD,CD)
      COMMON XI
      COMMON /CRK/ QD, XI1, CG
      COMPLEX G(4), A(4), B(4), XF, DX, AD, GIN, CD, CG
      EXTERNAL DLP,DLP1
      G(1) = 0.
      G(2) = 0.
      G(3) = GIN
      G(4) = 0.
      XF = XI
```

```
      CALL RKGC(DLP,G,XF,DX,A,B,4)
      G(3) = G(3) + QD + CG*G(2)
      IF (XI1.EQ.0.) GO TO 18
      XF = XI + XI1
      CALL RKGC(DLP1,G,XF,DX,A,B,4)
18    AD = G(3)
      CD = G(4)
      RETURN
      END

$IBFTC DRVLP
      SUBROUTINE DLP(G,GP)
      COMMON /CDR/ Q, GD
      COMMON XI
      COMPLEX GD,G(4),GP(4)
      T = REAL(G(1))
      GO TO 10
      ENTRY DLP1(G,GP)
      T = XI
10    GP(1) = 1.
      GP(2) = G(3)
      S = SQRT(1.+Q*T)
      GP(4) = G(2)/S
      GP(3) = G(2) - GD*(GP(4) + S)
      RETURN
      END

$IBFTC RKGHC
      SUBROUTINE RKGC (DERIV, Y, XFINAL, DELTA, Q, YP, N)
C  RUNGE-KUTTA-GILL INTEGRATION OF N-1 COMPLEX FUNCTIONS OF COMPLEX
C  ARGUMENT Y(1) FROM Y(1)INITIAL TO XFINAL
      DIMENSION A(4), B(4), C(4)
      COMPLEX Y(1), Q(1), YP(1), XFINAL, DELTA, T
      DATA A/.5, .292893219, 1.70710678, .166666667/, B/2., 1., 1., 2./,
     1     C/.5, .292893219, 1.70710678, .5/
      KK = CABS((XFINAL-Y(1))/DELTA) + .01
      IF (KK.LE.0) GO TO 20
      DO 5 I = 1, N
5     Q(I)=0.
      DO 10 K = 1, KK
      DO 10 J = 1, 4
      CALL DERIV(Y,YP)
      DO 10 I=1,N
      T=A(J)*(YP(I)-B(J)*Q(I))
      Y(I)=Y(I)+DELTA*T
10    Q(I)=Q(I)+3.*T-C(J)*YP(I)
20    RETURN
      END

$DATA
  190.  .5  1.  1.5 2.  3.  4.  5.  6.  8.  10. 15. 20. 30. 40. 50. 60. 80. 100.
 .75     .75      4.       5.       .4       .7       1.2
   3.  3.  3.  3.  4.  5.  6.  7.  9.  10. 12. 17. 22. 31. 41. 51. 61. 81. 100.
 .75     .75      4.       10.      .4       .7       1.2
   6.  8.  9.  9.  10. 11. 12. 13. 14. 15. 17. 21. 26. 35. 44. 53. 63. 82. 101.
```

Geometric configurations

σ estimates

Λ array

P-PERTURBATION ANALYSIS FOR HYBRID BEARING IN STEADY CIRCULAR WHIRL

L/D	L1/D	LAMBDA T	1+DELTA**2	K=CP/CV	ALFA	V=PS/PA	VC
0.750	0.750	4.000	1.200	1.400	0.700	5.000	0.400

SOLVE FOR YA = PC/V

1	YA	0.528282	DYA 0.459088E-01
2	YA	0.574191	DYA -0.285489E-02
3	YA	0.571336	DYA -0.112002E-04
4	YA	0.571324	DYA 0.186657E-08

PC/PS 0.571 PSO 0.640E-01 PS1 0.210 RKDX REDUCED UNTIL ERROR .LE. 0.500E-02

LAMBDA	FR/EPALD	FT/EPALD	W/EPALD	W/E(PS-PA)LD	PHI	MCW2/PALD	RKDX	WPC5/2LR5MU2	WHIRL RATIO	VIB NR SIGMA
0	2.352	-0.313E-06	2.3521	0.5880	-0.762E-05	0	0.1875	0	1000.0	0
0	2.389	-0.187E-01	2.3890	0.5973	-0.450	0	0.1875	38.223	1000.0	3.0000
0	2.415	0.108E-02	2.4149	0.6037	0.256E-01	0	0.1875	347.74	1000.0	1.0000
0	2.414	0.856E-03	2.4138	0.6034	0.203E-01	0	0.1875	282.73	1000.0	1.1088
0	2.409	-0.909E-03	2.4088	0.6022	-0.216E-01	0	0.1875	148.44	1000.0	1.5286
0	2.411	0.187E-03	2.4114	0.6029	0.444E-02	0	0.1875	201.60	1000.0	1.3124
LAMBDA	FR/EPALD	FT/EPALD	W/EPALD	W/E(PS-PA)LD	PHI	MCW2/PALD	RKDX	WPC5/2LR5MU2	WHIRL RATIO	VIB NR SIGMA
0.500	2.362	0.116	2.3647	0.5912	2.815	0	0.1875	0	0	0
0.500	2.336	0.623E-01	2.3365	0.5841	1.529	0.2595	0.1875	37.370	3.0000	3.0000
0.500	2.313	-0.118E-01	2.3125	0.5781	-0.292	0.9250E-01	0.1875	13.320	5.0000	5.0000
0.500	2.314	-0.160E-03	2.3140	0.5785	-0.397E-02	0.1056	0.1875	15.199	4.6822	4.6822
0.500	2.314	0.159E-05	2.3140	0.5785	0.393E-04	0.1058	0.1875	15.228	4.6778	4.5773
LAMBDA	FR/EPALD	FT/EPALD	W/EPALD	W/E(PS-PA)LD	PHI	MCW2/PALD	RKDX	WPC5/2LR5MU2	WHIRL RATIO	VIB NR SIGMA
1.000	2.390	0.228	2.4010	0.6003	5.433	0	0.1875	0	0	0
1.000	2.289	0.156	2.2943	0.5736	3.902	1.0173	0.1875	36.624	1.5000	3.0000
1.000	2.252	0.466E-01	2.2530	0.5632	1.185	0.3604	0.1875	12.974	2.5000	5.0000
1.000	2.258	-0.443E-01	2.2587	0.5647	-1.125	0.1844	0.1875	6.6367	3.5000	7.0000
1.000	2.253	-0.289E-02	2.2525	0.5631	-0.735E-01	0.2482	0.1875	8.9353	3.0125	5.0251
1.000	2.252	0.199E-03	2.2523	0.5631	0.506E-02	0.2539	0.1875	9.1393	2.9786	5.9571
LAMBDA	FR/EPALD	FT/EPALD	W/EPALD	W/E(PS-PA)LD	PHI	MCW2/PALD	RKDX	WPC5/2LR5MU2	WHIRL RATIO	VIB NR SIGMA
1.500	2.435	0.330	2.4572	0.6143	7.720	0	0.1875	0	0	0
1.500	2.252	0.262	2.2677	0.5669	6.646	2.2524	0.1875	36.039	1.0000	3.0000
1.500	2.193	0.115	2.1957	0.5489	3.007	0.7894	0.1875	12.630	1.6667	5.0000
1.500	2.200	-0.365E-02	2.1997	0.5499	-0.951E-01	0.4040	0.1875	6.4643	2.3333	7.0000
1.500	2.199	-0.534E-03	2.1990	0.5498	-0.139E-01	0.4111	0.1875	6.5774	2.3128	6.9385
1.500	2.199	0.307E-05	2.1989	0.5497	0.803E-04	0.4123	0.1875	6.5971	2.3093	6.9280
LAMBDA	FR/EPALD	FT/EPALD	W/EPALD	W/E(PS-PA)LD	PHI	MCW2/PALD	RKDX	WPC5/2LR5MU2	WHIRL RATIO	VIB NR SIGMA
2.000	2.493	0.421	2.5280	0.6320	9.578	0	0.1875	0	0	0
2.000	2.164	0.288	2.1826	0.5457	7.590	2.1635	0.1875	19.472	1.0000	4.0000
2.000	2.130	0.113	2.1331	0.5333	3.036	0.9467	0.1875	8.5206	1.5000	6.0000
2.000	2.154	-0.138E-01	2.1544	0.5386	-0.368	0.5386	0.1875	4.8473	2.0000	8.0000
2.000	2.151	-0.210E-02	2.1506	0.5377	-0.553E-01	0.5682	0.1875	5.1141	1.9454	7.7818
2.000	2.150	0.474E-04	2.1500	0.5375	0.125E-02	0.5738	0.1875	5.1644	1.9357	7.7427

Figure 8. - Example of working sheet.

P-PERTURBATION ANALYSIS FOR HYBRID BEARING IN STEADY CIRCULAR WHIRL

L/D	L1/D	LAMBDA I	1+DELTA**2	K=CP/CV	ALFA
0.750	0.750	4.000	1.200	1.400	0.700

V=PS/PA	CL.VOL.RAT.VC	PC/PS	PSO	PS1	RKEP
5.000	0.400	0.571	0.640E-01	0.210	0.500E-02

BRG NR LAMBDA	BRG LOAD W/EPALD	ATT ANGLE PHI	WHIRL RATIO W3/OMEGA	VIB NR SIGMA	STABILITY PARAMETERS MCW2/PALD	MPC5/2LR5W2
0	2.352	-0.762E-05	1000.	1.312	0	201.6
0.500	2.365	2.816	4.678	4.678	0.106	15.23
1.000	2.401	5.439	2.979	5.957	0.254	9.139
1.500	2.457	7.720	2.309	6.928	0.412	6.597
2.000	2.528	9.578	1.936	7.743	0.574	5.164
3.000	2.692	12.01	1.522	9.133	0.839	3.557
4.000	2.857	13.06	1.293	10.34	1.183	2.662
5.000	3.004	13.24	1.145	11.45	1.449	2.087
6.000	3.129	12.93	1.040	12.48	1.688	1.688
8.000	3.312	11.75	0.903	14.44	2.071	1.165
10.00	3.431	10.47	0.815	16.30	2.345	0.844
15.00	3.586	7.992	0.693	20.78	2.655	0.425
20.00	3.656	6.427	0.630	25.21	2.618	0.236
30.00	3.717	4.673	0.570	34.22	2.158	0.863E-01
40.00	3.745	3.732	0.543	43.48	1.654	0.372E-01
50.00	3.761	3.145	0.529	52.93	1.258	0.181E-01
60.00	3.773	2.740	0.521	62.51	0.970	0.970E-02
80.00	3.787	2.214	0.512	81.95	0.612	0.344E-02
100.0	3.797	1.880	0.508	101.6	0.414	0.149E-02

Figure 9. - Calculation summary sheet.

REFERENCES

1. Cunningham, Robert E.; Fleming, David P.; and Anderson, William J.: Experiments on Stability of Herringbone-Grooved Gas-Lubricated Journal Bearings to High Compressibility Numbers. NASA TN D-4440, 1968.

2. Gunter, E. J., Jr.; Hinkle, J. G.; and Fuller, D. D.: Design Guide for Gas-Lubricated, Tilting-Pad Journal and Thrust Bearings with Special Reference to High-Speed Rotors. Rep. 1-A2392-3-1, Franklin Inst. (AEC Rep. NYO-2512-1), Nov. 1964, p. 2.

3. Stewart, Warner L.; Anderson, William J.; Bernatowicz, Daniel T.; Guentert, Donald D.; Packe, Donald E.; and Rohlik, Harold E.: Brayton Cycle Technology. Space Power Systems Advanced Technology Conference. NASA SP-131, 1966, p. 106.

4. Lund, J. W.: A Theoretical Analysis of Whirl Instability and Pneumatic Hammer for a Rigid Rotor in Pressurized Gas Journal Bearings. J. Lubr. Tech., vol. 89, no. 2, Apr. 1967, pp. 154-166.

5. Pan, C. H. T.: Spectral Analysis of Gas Bearing Systems for Stability Studies. Dynamics and Fluid Mechanics. Vol. 3, Part 2 of Developments in Mechanics. T. C. Huang and M. W. Johnson, Jr., eds., John Wiley & Sons, Inc., 1965, pp. 431-447.

6. Lund, J. W.: The Hydrostatic Gas Journal Bearing with Journal Rotation and Vibration. J. Basic Eng., vol. 86, no. 2, June 1964, pp. 328-336.

7. Vohr, J. H.; and Chow, C. Y.: Characteristics of Herringbone-Grooved, Gas-Lubricated Journal Bearings. J. Basic Eng., vol. 87, no. 3, Sept. 1965, pp. 568-578.

8. Bisson, Edmond E.; and Anderson, William J.: Advanced Bearing Technology. NASA SP-38, 1964, p. 111.

9. Malanoski, S. B.: Experiments on an Ultrastable Gas Journal Bearing. J. Lubr. Tech., vol. 89, no. 4, Oct. 1967, pp. 433-438.

10. Anon.: Design of Gas Bearings. Vol. I: Design Notes. Mechanical Technology, Inc., 1966.

11. Cavicchi, Richard H.: Critical-Speed Analysis of Flexibly Mounted Rigid Rotors. NASA TN D-4607, 1968.

12. Gunter, Edgar J., Jr.: Dynamic Stability of Rotor-Bearing Systems. NASA SP-113, 1966, p. 21.

"The aeronautical and space activities of the United States shall be conducted so as to contribute . . . to the expansion of human knowledge of phenomena in the atmosphere and space. The Administration shall provide for the widest practicable and appropriate dissemination of information concerning its activities and the results thereof."

—NATIONAL AERONAUTICS AND SPACE ACT OF 1958

NASA SCIENTIFIC AND TECHNICAL PUBLICATIONS

TECHNICAL REPORTS: Scientific and technical information considered important, complete, and a lasting contribution to existing knowledge.

TECHNICAL NOTES: Information less broad in scope but nevertheless of importance as a contribution to existing knowledge.

TECHNICAL MEMORANDUMS: Information receiving limited distribution because of preliminary data, security classification, or other reasons.

CONTRACTOR REPORTS: Scientific and technical information generated under a NASA contract or grant and considered an important contribution to existing knowledge.

TECHNICAL TRANSLATIONS: Information published in a foreign language considered to merit NASA distribution in English.

SPECIAL PUBLICATIONS: Information derived from or of value to NASA activities. Publications include conference proceedings, monographs, data compilations, handbooks, sourcebooks, and special bibliographies.

TECHNOLOGY UTILIZATION PUBLICATIONS: Information on technology used by NASA that may be of particular interest in commercial and other non-aerospace applications. Publications include Tech Briefs, Technology Utilization Reports and Notes, and Technology Surveys.

Details on the availability of these publications may be obtained from:

SCIENTIFIC AND TECHNICAL INFORMATION DIVISION

NATIONAL AERONAUTICS AND SPACE ADMINISTRATION

Washington, D.C. 20546